

## FINITE ELEMENT STRESS ANALYSIS OF NONSPHERICAL COATED PARTICLES

K. DRITTLER

*Institut für Reaktorsicherheit der Technischen Überwachungs-Vereine e.V. (IRS), D-5 Köln, Germany  
(formerly at Institut für Reaktorwerkstoffe, Kernforschungsanlage Jülich, Jülich, Germany)*

I. GRIEGER

*Institut für Statik und Dynamik der Luft- und Raumfahrtkonstruktionen (ISD),  
Universität Stuttgart, D-7000 Stuttgart-Vaihingen, Germany*

### SUMMARY

In High Temperature Gas Cooled Reactors the fissile materials within the fuel elements are particles which are coated with several layers of substances which are capable of retaining fission products. In these layers stresses are created due to irradiation induced length changes as well as fission gas pressure. By increasing the irradiation time, the stresses reach such high values that these layers are destroyed.

There are several reasons why particles have to be used which deviate to some extent from the spherical shape. But the known theoretical investigations about the behaviour of irradiated coated particles all include the assumption that spherical symmetry exists.

Models of coated particles which are symmetrical with respect to an axis are analysed to study certain aspects of the influence of nonsphericity. Only the outer layers consisting of pyrolytic carbon, or a combination of pyrolytic carbon, silicon carbide and pyrolytic carbon are taken into account. It is assumed that only fission gas pressure acts upon the inner surface of these layers.

The inner and outer surfaces of the first kind of models have the shape of ellipsoids of revolution. The deviation of layer thicknesses from constant values was made as small as possible.

The inner surface of the second kind of models are assumed to be spherical, but by variation of the layer thickness the outer surfaces are adapted to characteristic forms often shown by manufactured coated particles.

The calculations were carried out using the Method of Finite Elements. The triangular curvilinear ring element TRIAXC6 of the code ASKA was chosen.

The investigated deviations from sphericity led to stresses whose absolute values are several times higher than those calculated for particles with spherical symmetry. A detailed analysis of the results can be summarized by the following rule: in general, strong but "locally" restricted deviations from the spherical shape (i.e. a bulge) induce less stresses than weak but "global" deformations (i.e. lenses).

## 1. Introduction

In order to reduce the number of parameters which have to be taken into account, research work on coated particles has been done more or less under the assumption that these particles have spherical symmetry. Up to now, the known theoretical investigations have not regarded deviations from the spherical shape. However, there are several reasons - mostly economic ones - why coated particles with a certain unsphericity have to be used in High Temperature Gas Cooled Reactors.

Simple considerations show that particles which are not spherically shaped fail at lower irradiation doses than those which are spherical (provided that their materials and designs are the same). Therefore, it would be of great practical value to know to what extent unsphericity of coated particles may be tolerable. However, in order to solve these problems immense difficulties are encountered.

The calculation of the distribution of stresses in certain coated particle models is one approach that can be used to obtain some information about these problems. The results of this calculation can be summarized in a rule which is of certain value for the fabrication of particles and for irradiation experiments dealing with coated particles that are not spherical.

## 2. Properties of the models

### 2.1 General remarks

In order to be able to investigate the behaviour of realistically shaped coated particles, the Finite Element Method for stress calculation was chosen. However, the analysis of very detailed coated particle models would be too extensive. Therefore two assumptions were made:

- the models of coated particles are symmetrical with respect to an axis (axisymmetric)
- the models consist only of an outer layer with an internal fission gas pressure

### 2.2 Geometric properties

For reasons of comparison, a hollow sphere as model layer was calculated (Fig.1). Besides this, two kinds of models were investigated:

- The inner and outer surfaces have the shapes of ellipsoids. The layer thickness at the farthest and nearest distance from the central point<sup>+)</sup>  are equal. (Fig. 2 and Fig. 3 show intersection curves)

---

<sup>+)</sup>  The middle point of the two focus points.

- The inner surfaces are spherical. The shapes of the outer surfaces were chosen to be similar to those which can often be seen from fabricated particles (Fig. 4 and Fig. 5 show intersection curves)

### 2.3 Coordinates

For the sake of simplicity all geometric and physical quantities are referred to the following local coordinate system:

- The radial coordinate (index r) has the radial direction which is strictly bound to the central point (for the second kind of models the central point is the middle point of the spherical inner surface)
- The first "tangential" coordinate (index t1) is vertical to the radial coordinate and lies in one plane with the axis of rotation
- The second "tangential" coordinate (index t2) is also vertical to the radial coordinate, but vertical to the axis of rotation as well (Fig. 6)

In general the radial and first tangential coordinates do not match the normal and tangential directions of the intersection curves from the outer and inner surfaces of the model layers.

These deviations, however, are only comparatively small since the shapes of the model layers are still not far from being a hollow sphere.

### 2.4 Material constants

The following elastic moduli were assumed for the layer material and represent pyrolytic carbon:

Young's Modulus in radial direction,

$$E_r = 2,0 \cdot 10^5 \text{ kp/cm}^2$$

Young's Modulus in tangential direction,

$$E_t = 2,5 \cdot 10^5 \text{ kp/cm}^2$$

Poisson's ratio  $\nu = 0,25$

### 2.5 Effects of radiation

Besides a fission gas pressure, P, which acts inside the layers, anisotropic radiation induced length changes are regarded. The relative length changes in radial and tangential direction have the symbols  $\epsilon_r$  and  $\epsilon_t$ .

### 2.6 Superposition

Since the linear elasticity theory is used, the effects of internal gas pressure and radiation induced length changes can be superposed. Therefore, the following formula for the stress components holds

$$\begin{aligned} \bar{\sigma}_{kl} &= P \cdot F_{kl} + (\epsilon_r - \epsilon_t) \cdot G_{kl} \quad ++ \\ kl &= rr, t1t1, t2t2, rt1 \quad (rt2, t1t2) \end{aligned} \quad (1)$$

The most general way to represent the results can be achieved by calculating with

$$\begin{aligned} \frac{\bar{\sigma}_{kl}}{P} &= F_{kl} + \frac{\epsilon_r - \epsilon_t}{P} G_{kl} \\ kl &= rr, t1t1, t2t2, rt1 \quad (rt2, t1t2) \end{aligned} \quad (2)$$

or

$$\begin{aligned} \frac{\bar{\sigma}_{kl}}{\epsilon_r - \epsilon_t} &= \frac{P}{\epsilon_r - \epsilon_t} F_{kl} + G_{kl} \\ kl &= rr, t1t1, t2t2, rt1 \quad (rt2, t1t2) \end{aligned} \quad (3)$$

### 2.7 Numerical method

Using the Finite Element Code ASKA [1], the stress distributions in the model layers were calculated for several specific cases of internal pressure and irradiation induced length changes.

In order to get an extreme low number of nodal points in the curves of intersections, the ring element TRIAXC6 with curvilinear boundaries [1] was taken.

(The validity of the superposition described in section 2.6 can be shown from the results).

Since a large amount of stress values were obtained, the stress distribution was scored automatically by an interactive graphic screen [2], [3]

### 2.8 Presentation of the results

The considerations within this report are restricted to the stress distributions at the outer surfaces of the model layers. This is the simplest way to connect the surface lines of the geometric shapes of the model layers with the representations of the stress distributions in one figure. The stresses are evaluated for the coordinate system described in section 2.3. Referring to the curves of intersection, the stress components are drawn in radial directions starting from those nodal points at the corners of the TRIAXC6 elements which lie in the outer boundaries of the model layers. These stress component coordinates are connected with straight lines. In this way the screen scores were obtained, photographs of which are reproduced in Fig. 7 to 16.

In order to get more general results the explanations of the figure captions use reduced stress components (section 2.6).

<sup>+</sup>For the isotropic case, in which the relation  $\epsilon_r = \epsilon_t$  is valid, the second term must vanish.

### 3. Discussion of the results

Table 1 lists the ratios of the maximum amounts of all stresses in the outer surfaces of the model layers and the stress in the outer surface of the hollow sphere. Within this table it is seen that in the case of irradiation induced length changes the stresses in the outer surfaces can be about 1.5 times the stress in the outer surface of the hollow sphere. The stresses in the outer surface of model layer 3 (ellipsoid 2) can have a factor 2.

In the case of internal gas pressure the stresses in the outer surfaces exceed that of a hollow sphere by a factor of 1,8 to 5. This means that geometric deviations from sphericity are more sensitive in the case of internal gas pressure than in the case of irradiation induced length changes. This sensitivity is especially strong in the case of the two ellipsoids (model layer 2 and 3).

Concluding these results in a more general way it can be said that comparatively strong but "locally" restricted deviations from the spherical shape (i.e. a bulge) induce less stresses in the outer surfaces than comparatively weak but "global" deformations (i.e. lenses).

This conclusion could be established for several examples of stress distributions in the model layers.

#### Acknowledgment

The authors would like to thank Mr. G. Wagemann for valuable help.

#### References

- 1 ANKA - Automatic System for Kinematic Analysis. User's Reference Manual, ISD Report No 73, Stuttgart, 1971
- 2 Grieger, I.: Über den Einsatz von Bildschirmgeräten bei der Berechnung von Tragwerken. Dr.-Ing.Dissertation, Universität Stuttgart, 1972
- 3 Grieger, I.: INGA-Interaktive graphische Analyse, Benutzerhandbuch, ISD-Bericht Nr. 135, Stuttgart, 1973

Table 1

The ratios (Q) of the maximum amounts of all stress components in the outer surfaces of the model layers and the stress in the outer surface of the hollow sphere (model layer 1, Fig. 1)

| Q<br>model layer                                    | model layer 2<br>(Fig. 2) | model layer 3<br>(Fig. 3) | model layer 4<br>(Fig. 4) | model layer 5<br>(Fig. 5) |
|---|---------------------------|---------------------------|---------------------------|---------------------------|
| Q in the case of irradiation induced length changes | 1,6                       | 2,0                       | 1,6                       | 1,5                       |
| Q in the case of internal gas pressure              | 2,4                       | 5,0                       | 1,8                       | 1,8                       |

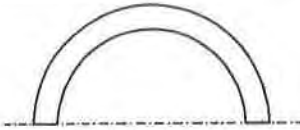


Fig. 1: Intersection curve of model layer 1 with axis of rotation (hollow sphere; radius of outer sphere; radius of inner sphere equal 5:4)

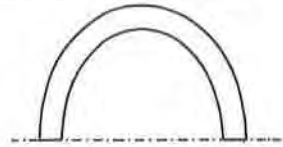


Fig. 2: Intersection curve of model layer 2 with axis of rotation (ellipsoid 1)

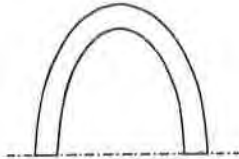


Fig. 3: Intersection curve of model layer 3 with axis of rotation (ellipsoid 2)

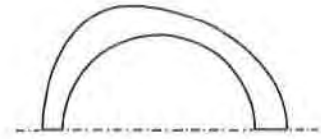


Fig. 4: Intersection curve of model layer 4 with axis of rotation (inner surface like in Fig. 1)

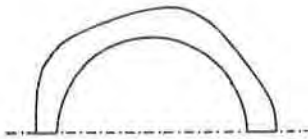


Fig. 5: Intersection curve of model layer 5 with axis of rotation (inner surface like in Fig. 1)

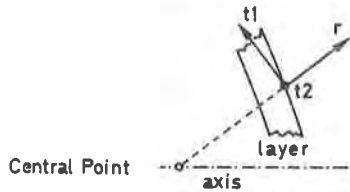


Fig. 6: System of coordinates; r, t1, t2 (vertical to the paper plane)

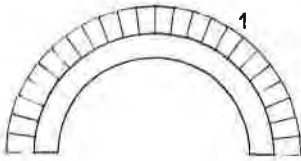


Fig. 7: Stress distribution in the outer surface of model layer 1 (hollow sphere, Fig. 1). Curve 1:  $\bar{\sigma}_{t1t1}/(\epsilon_r - \epsilon_t)$  and  $\bar{\sigma}_{t2t2}/(\epsilon_r - \epsilon_t)$ . The marked distance represents the stress of  $1 \text{ kp/mm}^2$  for  $\epsilon_r - \epsilon_t = 1$

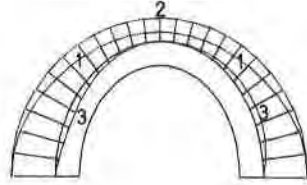


Fig. 8: Stress distribution in the outer surface of model layer 2 (ellipsoid 1, Fig. 2). Curve 1:  $\bar{\sigma}_{t1t1}/(\epsilon_r - \epsilon_t)$ ; curve 2:  $\bar{\sigma}_{t2t2}/(\epsilon_r - \epsilon_t)$ ; curve 3:  $\bar{\sigma}_{rt1}/(\epsilon_r - \epsilon_t)$ . The marked distance represents the stress of  $1 \text{ kp/mm}^2$  for  $\epsilon_r - \epsilon_t = 1$

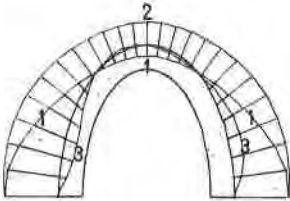


Fig. 9: Stress distribution in the outer surface of model layer 3 (ellipsoid 2, Fig. 3). curve 1:  $\bar{\sigma}_{t1t1}/(\epsilon_r - \epsilon_t)$ ; curve 2:  $\bar{\sigma}_{t2t2}/(\epsilon_r - \epsilon_t)$ ; curve 3:  $\bar{\sigma}_{rt1}/(\epsilon_r - \epsilon_t)$ . The marked distance represents the stress of  $1 \text{ kp/mm}^2$  for  $\epsilon_r - \epsilon_t = 1$

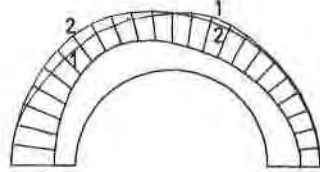


Fig. 10: Stress distribution in the outer surface of model layer 4 (Fig. 4). Curve 1:  $\bar{\sigma}_{t1t1}/(\epsilon_r - \epsilon_t)$ ; curve 2:  $\bar{\sigma}_{t2t2}/(\epsilon_r - \epsilon_t)$ . The marked distance represents the stress of  $1 \text{ kp/mm}^2$  for  $\epsilon_r - \epsilon_t = 1$

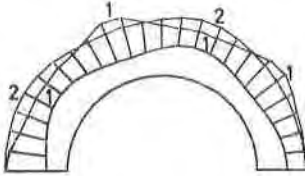


Fig. 11: Stress distribution in the outer surface of model layer 5 (Fig. 5).  
 Curve 1:  $\bar{\sigma}_{t1t1}/(\epsilon_r - \epsilon_t)$ ;  
 curve 2:  $\bar{\sigma}_{t2t2}/(\epsilon_r - \epsilon_t)$ .  
 The marked distance represents the stress of 1 kp/mm<sup>2</sup> for  $\epsilon_r - \epsilon_t = 1$

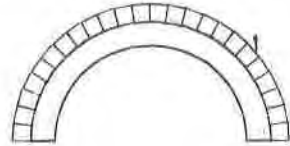


Fig. 12: Stress distribution in the outer surface of model layer 1 (hollow sphere, Fig. 1). Curve 1:  $\bar{\sigma}_{t1t1}/P$  and  $\bar{\sigma}_{t2t2}/P$ .  
 The marked distance represents the stress of 1 kp/mm<sup>2</sup> for  $P = 10^4$  kp/cm<sup>2</sup>.

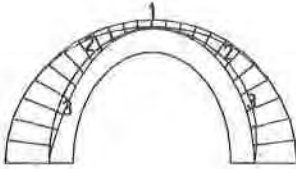


Fig. 13: Stress distribution in the outer surface of model layer 2 (ellipsoid 1, Fig. 2).  
 Curve 1:  $\bar{\sigma}_{t1t1}/P$ ,  
 curve 2:  $\bar{\sigma}_{t2t2}/P$ ,  
 curve 3:  $\bar{\sigma}_{rt1}/P$ .  
 The marked distance represents the stress of 1 kp/mm<sup>2</sup> for  $P = 10^4$  kp/cm<sup>2</sup>.

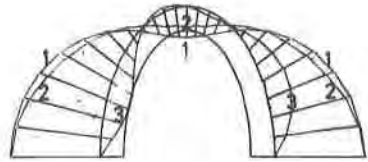


Fig. 14: Stress distribution in the outer surface of model layer 3 (ellipsoid 2, Fig. 3).  
 Curve 1:  $\bar{\sigma}_{t1t1}/P$ ,  
 curve 2:  $\bar{\sigma}_{t2t2}/P$ ,  
 curve 3:  $\bar{\sigma}_{rt1}/P$ .  
 The marked distance represents the stress of 1 kp/mm<sup>2</sup> for  $P = 10^4$  kp/cm<sup>2</sup>.

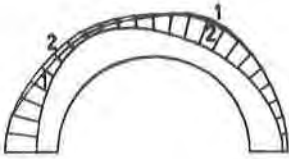


Fig. 15: Stress distribution in the outer surface of model layer 4 (Fig. 4).  
Curve 1:  $\bar{\sigma}_{t1t1}/P$ ,  
curve 2:  $\bar{\sigma}_{t2t2}/P$ .

The marked distance represents the stress of  $1 \text{ kp/mm}^2$  for  $P = 10^4 \text{ kp/cm}^2$

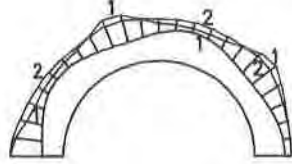


Fig. 16: Stress distribution in the outer surface of model layer 5 (Fig. 5).  
Curve 1:  $\bar{\sigma}_{t1t1}/P$ ,  
curve 2:  $\bar{\sigma}_{t2t2}/P$ .

The marked distance represents the stress of  $1 \text{ kp/mm}^2$  for  $P = 10^4 \text{ kp/cm}^2$ .

